Volume 1 | Number 1 | Jan 2013 | Pages 1–100

Dalton Transactions

An international journal of inorganic chemistry
www.rsc.org/dalton

ROYAL SOCIETY OF CHEMISTRY

ROYAL SOCIETY OF CHEMISTRY

www.rsc.org/dalton

Table of Contents

Syntheses, structures and properties of two new organic-inorganic materials based on ε-Zn Keggin units {ε-PMo$^V_8$Mo$^{VI}_4$O$_{40-x}$(OH)$_x$Zn$_4$}

Hao Miao[a], **Gonghao Hu**[a], **Jiuyu Guo**[a], **Hongxiang Wan**[a], **Hua Mei**[a,]*, **Yu Zhang**[a] and **Yan Xu**[a b]*
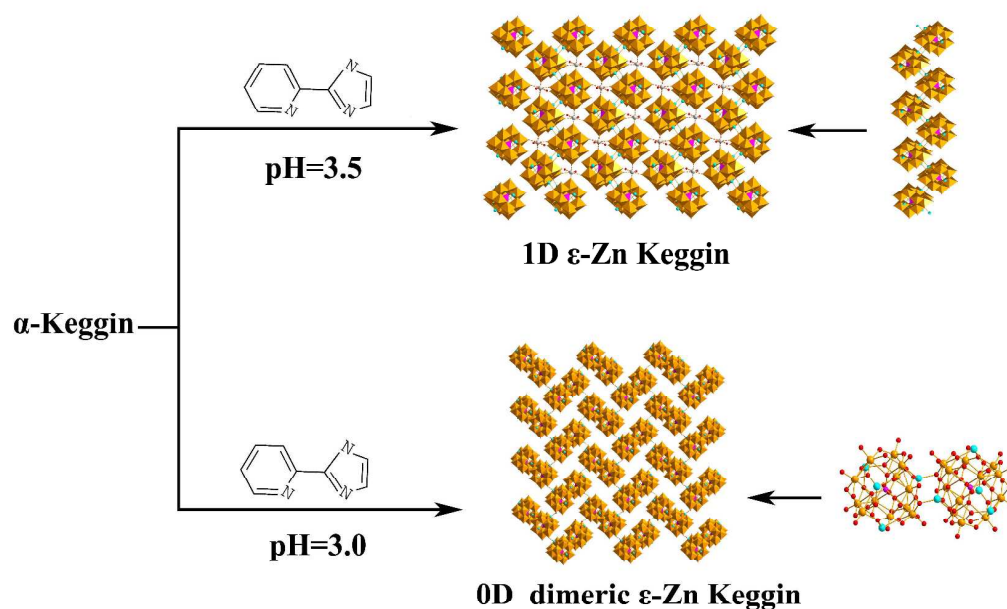
Two novel organic-inorganic hybrids, Na[PMo$^V_8$Mo$^{VI}_4$O$_{38}$(OH)$_2$Zn$_4$][pyim]$_2$·1.5H$_2$O [**ε(pyim)$_2$**] (pyim = 2-(2-Pydidyl)-imidazole) and [PMo$^V_8$Mo$^{VI}_4$O$_{37}$(OH)$_3$Zn$_4$]$_2$[pyim]$_6$·4H$_2$O [**ε$_2$(pyim)$_6$**], based on ε-Zn Keggin units {ε-PMo$^V_8$Mo$^{VI}_4$O$_{40-x}$(OH)$_x$Zn$_4$} have been successfully synthesized under hydrothermal conditions by controlling pH values. **ε(pyim)$_2$** is a 1D material with monomeric ε-Zn units modified by pyim ligands, while **ε$_2$(pyim)$_6$** is an isostructural compound with dimeric ε-Zn units modified by pyim ligands, which is the first isolated structure in the dimeric ε-Zn POMs.

Syntheses, structures and properties of two new organic-inorganic hybrid materials based on ε-Zn Keggin units {ε-PMo$^{V}_8$Mo$^{VI}_4$O$_{40-x}$(OH)$_x$Zn$_4$}

Hao Miao[a], **Gonghao Hu**[a], **Jiuyu Guo**[a], **Hongxiang Wan**[a], **Hua Mei**[a,*],

Yu Zhang[a] **and Yan Xu**[*a b]

Two novel organic-inorganic hybrids, Na[PMo$^{V}_8$Mo$^{VI}_4$O$_{38}$(OH)$_2$Zn$_4$][pyim]$_2$·1.5H$_2$O [**ε(pyim)$_2$**] (pyim = 2-(2-Pydidyl)-imidazole) and [PMo$^{V}_8$Mo$^{VI}_4$O$_{37}$(OH)$_3$Zn$_4$]$_2$[pyim]$_6$·4H$_2$O [**ε$_2$(pyim)$_6$**], based on ε-Zn Keggin units {ε-PMo$^{V}_8$Mo$^{VI}_4$O$_{40-x}$(OH)$_x$Zn$_4$} have been successfully synthesized under hydrothermal conditions by controlling pH values. Structural analysis indicates that the framework of **ε(pyim)$_2$** is a 1D chains constructed by monomeric ε-Zn units modified by pyim ligands. While **ε$_2$(pyim)$_6$** is an isolated structural compound with dimeric ε-Zn units modified by pyim ligands, which is the first isolated structure in the ε-keggin POMs system. The luminescent and electrochemical properties of **ε(pyim)$_2$** and **ε$_2$(pyim)$_6$** were investigated. **ε$_2$(pyim)$_6$** also shows high catalytic activity for the esterification of phosphoric acid with equimolar lauryl alcohol to monoalkyl phosphate ester (MAP).

[a]*College of Chemistry and Chemical Engineering, State Key Laboratory of Materials-oriented Chemical Engineering, Nanjing Tech University, Nanjing 210009, P.R. China. E-mail: yanxu@njtech.edu.cn; Tel:+86-25-83587857*

[b]*State Key Laboratory of Coordination Chemistry, Nanjing University, Nanjing 210093, P. R. China*

Introduction

Polyoxometalates (POMs) are one of the most widely used inorganic polydentate building blocks not only due to their extreme variability of compositions, molecular characteristics, but also their application in catalysis, photochemistry, gas storage and separation. [1-4] The combination of the properties of POMs with their varying coordination modes, together with a number of their ability to form organic-inorganic hybrids with transition metal complex or lanthanide complex moieties, provides an impetus for the synthesis of these multifunctional materials.[5-9]

The Keggin structure $\{XM_{12}O_{40}\}$ that is built from the association of a central XO_4 tetrahedron around by four M_3O_{13} groups, where X is the heteroatom (most commonly Si or P) and M is a transition metal ion in octahedral coordination with a high oxidation state is the most archetypal POM structure. Theoretically possible five geometrical isomers of the Keggin structure designated by the prefixes α, β, γ, δ, and ε are resulted from the serial 60° rotations around the 3-fold axes of the M_3O_{13} units have been reported by Baker and Figgis.[10] Interestingly, the ε-keggin POMs have always been observed encountered with four capping centers.

In the past decade, there have been only a few reports about the hybrid polyoxomolybdates based on a mixed-valence ε-Keggin unit. $\{\varepsilon\text{-PMo}^V_8\text{Mo}^{VI}_4\text{O}_{40-x}(\text{OH})_x\text{M}_4\}$ which is a versatile building unit, with M being either a zinc ion or a lanthanum ion located at the vertices of a mildly distorted tetrahedron. The charge of the Keggin unit lies on the number of protonated oxo bridging ligands varying from 0 to 5. Depending on their geometric orientation and the number of coordination sites, POMs can be functionalized by organic linkers easily either by direct connecting to the oxygen atoms of the POM or via rare earth or transition metal ions grafted at the surface of the POM.[11-13] Various organic linkers such as bipyridine,[14-16] benzenedicarboxylic acid,[17] imidazole,[18] trimesic acid [19] and para-azobipyridine,[20] have been successfully to the react of the ε-Keggin ions leading to a new family of 1D~3D materials. Additionally, these materials can display interesting magnetic, optical and catalytic properties, [21-23] although only a few reports

have discussion of their electrochemical behavior.[24, 25] As the isolated structure of POMs have better electrochemical properties and catalytic activity, it is therefore vital to design isolated novel ε-Keggin POM.

We describe herein the synthesis and characterization of two novel polyoxometalates $Na[PMo^V_8Mo^{VI}_4O_{38}(OH)_2Zn_4][pyim]_2 \cdot 1.5H_2O$ **ε(pyim)₂** and $[PMo^V_8Mo^{VI}_4O_{37}(OH)_3Zn_4]_2[pyim]_6 \cdot 4H_2O$ **ε₂(pyim)₆** containing monomeric, chain-like and dimeric, isolated ε-Zn Keggin building blocks connected by pyim ligands. It is noted that **ε₂(pyim)₆** was obtained with a isolated structure built of a dimerized ε-Zn Keggin when the pH value was lowered slightly. One of the biggest differences in the synthesis between everyone else and ours is that the ε-Keggin ions originate from the self-assembly of molybdenum powder or molybdate with phosphoric acid or phosphorous acid in others, while ε-Keggin ions of our hybrid polyoxometalates come from the configuration transformation from α-Keggin. Still, it is striking that there is no example of isolated cluster of dimerized ε-Keggin POM. Besides the structural data, the fluorescence properties and electrochemical properties of the two materials has thus been investigated. More interestingly, **ε₂(pyim)₆** shows high catalytic activity for the esterification of phosphoric acid with equimolar lauryl alcohol to monoalkyl phosphate ester (MAP).

Experimental section

Materials and physical methods

2-(2-Pydidyl)-imidazole was prepared according to the literature,[26] while other chemical reagents were commercially available and used without further purification. C, H, N elemental analyses were performed on Perkin-Elmer 2400 CHN elemental analyzer. IR spectra of all compounds were recorded with a Nicolet Impact 410 FTIR spectrometer using pressed KBr pellets in the 4000–450 cm^{-1} region. TG measurement was carried out on a Diamond thermogravimetric analyzer in flowing N_2 atmosphere from 25 to 800 °C with a heating rate of 10 °C min^{-1}. Solid state fluorescence properties of **ε(pyim)₂** and **ε₂(pyim)₆** were carried out using an F-4600

FL Spectrophotometer. Powder XRD patterns were obtained on Bruker D8X diffractometer equipped with monochromatized Cu-Kα ($\lambda = 0.15418$ nm) radiation at room temperature, and the data were collected in the range of $5\,° \leq 2\theta \leq 50\,°$. A CHI 440 electrochemical quartz crystal microbalance connected to a Digital-586 personal computer was used for the electrochemical experiments. A conventional three-electrode cell was used at room temperature. A saturated calomel electrode (SCE) was used as the reference electrode and a platinum wire as the counter electrode. The compounds **ε(pyim)$_2$** and **ε$_2$(pyim)$_6$** bulk-modified carbon paste electrodes (**ε(pyim)$_2$**–CPE and **ε$_2$(pyim)$_6$**–CPE) were used as the working electrodes.

Synthesis of Na[PMo$^V_8$Mo$^{VI}_4$O$_{38}$(OH)$_2$Zn$_4$][pyim]$_2$·1.5H$_2$O (ε(pyim)$_2$)

A mixture of Zn(OAC)$_2$·2H$_2$O (0.1103 g, 0.50 mmol), H$_3$PMo$_{12}$O$_{40}$·xH$_2$O (0.4452 g, 0.21 mmol) were dissolved in 8 mL of distilled water. The mixture was stirred for 2 h at room temperature and the pH of the mixture was adjusted to 3.5 with 6 M NaOH. Then a solution of pyim (0.0366 g, 0.25 mmol) in 4ml alcohol with stirring for 0.5 h was added. The suspension was put into a 20 mL Teflon-lined stainless-steel autoclave and kept under autogenous pressure at 170 °C for 4.5 days. After slow cooling to room temperature, black block crystals were filtered and washed with distilled water (28.81 % yield based on Mo). Elemental analysis (%) calcd (found) for **ε(pyim)$_2$**: C 7.92(7.88), H 0.79(0.72), N 3.46(3.43). IR (solid KBr pellet, cm^{-1}): 3448 (s), 1611 (m), 1470 (w), 1378(m), 1105 (m), 938 (s), 818 (m), 777 (s), 691(w), 546(w).

Synthesis of [PMo$^V_8$Mo$^{VI}_4$O$_{37}$(OH)$_3$Zn$_4$]$_2$[pyim]$_6$·4H$_2$O (ε$_2$(pyim)$_6$)

The synthesis procedure for **ε$_2$(pyim)$_6$** is similar to **ε(pyim)$_2$**, except for pH = 3.0. After slow cooling to room temperature, black block crystals were filtered and washed with distilled water (58.82 % yield based on Mo). Elemental analysis (%) calcd (found) for **ε(pyim)$_2$**: C 11.27(11.11), H 1.10(1.02), N 4.93(4.95). IR (solid KBr pellet, cm^{-1}): 3450 (s), 1618 (s), 1570(w), 1469 (s), 1382(m), 1294(w), 1106 (w), 937 (s), 822 (m),775 (s), 681(w), 540(w).

X-Ray crystallography

The single-crystal XRD data of **ε(pyim)₂** and **ε₂(pyim)₆** were obtained from a Bruker Apex II CCD with Mo-Kα radiation (λ = 0.71073 Å) at 296 K using ω-2θ scan method. The crystal structures were solved by direct method and refined by the full-matrix least-squares methods on F2 using the SHELX-97 program package. All of the non-hydrogen atoms were refined anisotropically. The hydrogen atoms of organic ligands were refined in calculated positions, assigned isotropic thermal parameters, and allowed to ride on their parent atoms, while the H atoms for O-H and water were not located. A summary of the crystallographic data and structural determination for both compounds is provided in Table 1.

Results and discussion

Synthesis

Hydrothermal synthesis has recently been proved to be a powerful method in the synthesis of POM-based organic-inorganic hybrid compounds. Many factors can affect the nucleation and crystal growth of final products during a specific hydrothermal synthesis, such as the type of initial reactants, starting concentrations of reactants, time, pH values, solvents and temperature. In our case, pH of the solution plays an important role for the formation of two compounds based on the ε-Zn Keggin units with different structures. In our parallel experiments, we only get powder impurities without crystals under a pH above 4 or below 3. Dimerized 0D ε-Zn Keggin **ε₂(pyim)₆** was obtained when the pH value was lowered slightly from 3.5 to 3.0. The ligand pyim was instead of the ligand imidazole and triazole in our parallel experiments. We only got some precipitations, also pyim may have the structure-directing role in the crystallization process of two compounds. It is also worth mentioning that the biggest differences in the synthesis is that the ε-Keggin ions of two compounds come from the configuration transformation from α-Keggin structural compounds, while originating from the self-assembly of molybdenum powder or molybdate with phosphoric acid or phosphorous acid in others.

PXRD analyses

PXRD measurements for **ε(pyim)₂** and **ε₂(pyim)₆** were determined at room temperature (Figure S1 and S2), the diffraction peak positions of the experimental XRD patterns of **ε(pyim)₂** and **ε₂(pyim)₆** are in accordance with that of simulated XRD patterns, indicating the phase purity of the two compounds.

IR spectra

The infrared spectra of **ε(pyim)₂** and **ε₂(pyim)₆** are similar (Figure S3 and S4). Take **ε₂(pyim)₆** as example, several regions can be differentiated: Typical absorption characteristic peaks for 2-(2-pyridyl)-imidazole are found around $1150-1611$ cm^{-1}. The signature of Mo$-$O and P$-$O vibrations of the inorganic skeleton of the **ε-POM** are identified around 938 and 1105 cm^{-1} respectively, while the Mo$-$O$-$Mo vibrations are encountered below 938 cm^{-1}. In addition, O$-$H vibrations is found around 3448 cm^{-1}.

Crystal structure of 1

The two hybrid materials are based on the well-known {ε-PMo$^{V}_8$Mo$^{VI}_4$O$_{40}$Zn$_4$} POM unit, a reduced ε-Keggin isomer capped by four transition ions Zn(II) in tetrahedral coordination on its surface. In the structures of ε-Zn derivatives, [27] the ε-PMo$_{12}$ Keggin isomer, containing 8 Mo(V) and 4 Mo(VI) ions is an eight-electron reduced POM, as confirmed by the examination of the Mo(V)-Mo(V) bonds (ca. 2.6 Å) and Mo(VI)-Mo(VI) bonds (ca. 3.2 Å), as well as bond valence sum calculations on the Mo centers (Table S1 in Supporting Information). Indeed, valence bond calculations figure clearly that Mo3, Mo5, Mo8 and Mo10 are Mo(V) ions, also in agreement with their intermetallic Mo-Mo bonds.

Two different coordination modes are encountered in **ε(pyim)₂**. Thus, Zn1 and Zn2 both are tetra-coordinated in a tetrahedron coordination geometry, being bound to three oxygen atoms of one ε-Keggin core and one oxygen atom of another **ε**-Keggin

core, Zn3 and Zn4 both bound to three oxygen atoms of one ε-Keggin core, two nitrogen atom of a pyim ligand, and are thus penta-coordinated in a square-pyramidal coordination geometry (Figure 1).

In **ε(pyim)₂**, the zigzag chain of POM building block can be seen as the condensation of {ε-PMo$^V_8$Mo$^{VI}_4$O$_{40}$Zn$_4$} POMs via Zn-O bonds (1.944(6)-2.275(9) Å) with two adjacent POMs. Such condensation has also been evidenced in the chain built of previously reported [**ε(trim)**]$_\infty$ [19] and molybdogermanate ε-Keggin POMs {GeMo$^V_8$Mo$^{VI}_4$O$_{36}$(OH)$_4$Ni$_4$}.[28] Due to the pyim was used, the conformation of [PMo$^V_8$Mo$^{VI}_4$O$_{38}$(OH)$_2$Zn$_4$pyim$_2$]$_n$ chain in **ε(pyim)₂** is much different. Then, adjacent 1D zigzag chains are liked up to yield a 2D net structure via Na-O bonds with the average bond length 2.491(5) Å and each sodium atom connects to the four adjacent POMs (Figure 2). Free water molecules partake in the strong H-bonding interactions with the polyanion framework and are filled in the cavities of 3D supramolecular architecture.

Crystal structure of 2

Slight variations in the conditions of experimental synthesis had strong influences on the structures of the compounds affording another phase, **ε₂(pyim)₆**. Examination of the Mo···Mo distances and valence bond calculations (Table S1 in Supporting Information) have confirmed the presence of eight Mo(V), four Mo(VI) ions and three bridging oxygen atoms are protonated. Differently, the inorganic building unit in **ε₂(pyim)₆** is a dimerized form of **ε**-Zn POM, resulting from the condensation of two **ε**-Zn POM units through the formation of two Zn–O bonds between one capping Zn(II) ion on a **ε**-Zn POM unit and a bridging oxygen atom of an adjacent **ε**-Zn POM (Figure 3).

The dimer has already been described in **ε₂(pazo)₄**,[11] **ε₂(im)₄**,[9] and **ε₂(trim)₂**,[8] which are 1D, 2D and 3D respectively. In **ε₂(pazo)₄**, the two Zn^{II} ions on the dimeric **ε**-Zn POMs are bound to one O atom of a free HPO$_3^{2-}$ ion, being from the H$_3$PO$_3$ precursor, which allows the connection of the dimers into a 1D chain. While in **ε₂(im)₄**, the two Zn^{II} ions on the dimeric **ε**-Zn POMs are coordinated to bridging

imidazolate ligands that ensure the connection of the dimeric ε-Zn POMs to four adjacent dimers thus leading to the formation of **ε₂(im)₄** into a 2D layers structure. The 3D framework of **ε₂(trim)₂** is generated by the connection of the dimeric ε-Zn POMs and the bifunctionality of the organic ligand. Since the pyim was used, we have fortunately synthesized the first isolated structure in the family of dimerized form of ε-Zn POMs. It follows that this dimeric ε-Zn POM possesses six accessible capping Zn(II) ions and four of them are chelated by a pyim ligand respectively. The connection of the dimeric ε-Zn POMs via H-bonding interactions generates a 3D supramolecular framework that stack up in a windmill type along the a axis (Figure 4).

Although our experimental structures of **ε(pyim)₂** and **ε₂(pyim)₆** are not Z-POMOF type structures, the synthesis of **ε(pyim)₂** shows that pyim ligands can also connect ε-Zn POMs and the successful synthesis of **ε₂(pyim)₆** verify the dimerized form of ε-Zn POMs can also be isolated structures. Our experimental structures suggest that a Z-POMOF structure with pyim ligands could be obtained through varying the synthetic conditions particularly in pH and temperature in our future work.

Fluorescence spectrum

The luminescence studies of **ε(pyim)₂** and **ε₂(pyim)₆** and the ligand pyim are explored in the solid state at room temperature. The emission bands are centered at about 370 nm for imidazole, which may attributed to the ligand-centered π^*-π electronic transitions. Comparably, **ε(pyim)₂** and **ε₂(pyim)₆** exhibit similar emission band at ca. 398 nm and 400 nm upon excitation at 597 and 600 nm (Figure S5 and S6). Clearly, the emission spectra of **ε(pyim)₂** and **ε₂(pyim)₆** are both red-shifted compared with the free pyim ligands, which may be attributed to the charge-transition between ligands and metal ion centers. In comparison with free organic ligands, the emission intensity increases as the rigidity of the ligands is increased by reducing the loss of energy through thermal vibrations through the hydrogen bonding interactions between the organic ligands and the guest water molecular.

Voltammetric behavior

The electrochemical behaviour of $\varepsilon(pyim)_2$ and $\varepsilon_2(pyim)_6$ have been investigated in a 1 M H_2SO_4 aqueous solution at different scan rates. The bulk-modified CPE which is easy to prepare and handle becomes a good optimal choice to study the electrochemical properties as $\varepsilon(pyim)_2$ and $\varepsilon_2(pyim)_6$ are insoluble in water and common organic solvents. The CV plot for $\varepsilon(pyim)_2$–CPE and $\varepsilon_2(pyim)_6$–CPE in a 1 M H_2SO_4 aqueous solution at different scan rates is presented in Figure. 5 and 6.

Three reversible redox peaks (I–I′, II–II′, III–III′) appear in the potential range of -200 to 800 mV in both $\varepsilon(pyim)_2$ and $\varepsilon_2(pyim)_6$. The mean peak potentials ($E_{1/2} = (E_{pa} + E_{pc})/2$) for $\varepsilon(pyim)_2$ are 366 mV, 181 mV and -43 mV respectively and for $\varepsilon_2(pyim)_6$, the mean peak potentials are 357 mV (I–I′), 200 mV (II–II′) and -42 mV (III–III′) which could be ascribed to the redox progress of $Zn^{II/0}$ and $Mo^{VI/V}$. In addition, there pairs of reversible redox peaks I–I′, II–II′ and III–III′ can be ascribed to three consecutive two-electron processes.[29, 30] The peak potentials change gradually along with the scan rates from 80 to 400 mV s^{-1} for $\varepsilon(pyim)_2$ and from 20 to 200 mV s^{-1} for $\varepsilon_2(pyim)_6$: The anodic peak potentials transfer to the positive direction and the corresponding cathodic peak potentials shift toward the negative direction with increasing scan rates.
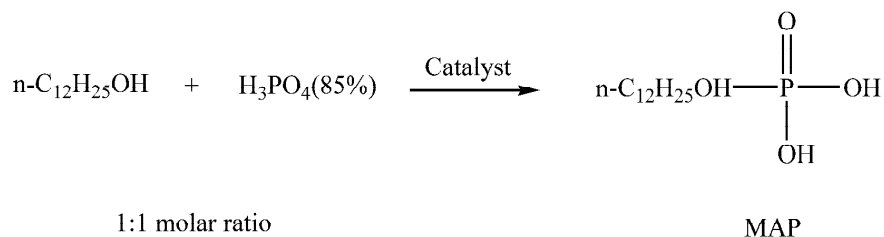
Thermogravimetric analyses

The thermal behaviors of $\varepsilon(pyim)_2$ and $\varepsilon_2(pyim)_6$ were investigated on crystalline samples under N_2 atmosphere from 25 to 800 ℃. The TG curve (Figure S7) of $\varepsilon(pyim)_2$ shows a slight weight loss of 1.13% before 180 ℃ corresponds to the release of 1.5 lattice water molecules (calc. 1.11%). The second weight loss of 13.13% from 140 to 440 ℃ is assigned to the removal of all pyim ligands and the dehydration of two hydroxyl groups (calc. 13.37%). The TG curve (Figure S8) of $\varepsilon_2(pyim)_6$ is similar to that of $\varepsilon(pyim)_2$, also exhibits two weight loss steps. The first weight loss of 1.45% between 25 to 150 ℃ corresponds to the release of 4 lattice water molecules (calc. 1.41%). The second weight loss of 19.17% between 195 to

700 ℃ is assigned to the removal of all pyim ligands and the dehydration of six hydroxyl groups (calc. 13.37%).

Catalytic activity experiment

The esterification of phosphoric acid with equimolar lauryl alcohol (Scheme 1) was performed in a 100 ml three-necked round-bottomed flask fitted in a Dean-Stark trap (toluene was heated to reflux to remove water) and a magnetic stirrer. A solution of **ε₂(pyim)₆** (0.095 g), phosphoric acid (0.067 mol, 85% aqueous solution), and lauryl alcohol (0.067 mol) in toluene (15 ml) were charged into the flask and the mixture was heated at 110 °C for 25 h under stirring while maintaining gentle reflux. After quenching the reaction, the product mixture was diluted with the water (5 ml) and isopropanol (5 mL), transferred into a separating funnel and allowed to settle for one hour. The supernatant oil layer was then separated directly from the mixture and evaporated on a rotary evaporator under 90 ℃ until dry. The yield and selectivity of MAP in the product mixture were determined by potentiometric titration ground on the amount of phosphoric acid in the starting reactants with the three different dissociation constants of H_3PO_4 .[31, 32]

$$\text{n-}C_{12}H_{25}OH \quad + \quad H_3PO_4(85\%) \xrightarrow{\text{Catalyst}} \quad \text{n-}C_{12}H_{25}OH\!-\!\!\!\underset{\underset{OH}{|}}{\overset{\overset{O}{\|}}{P}}\!\!\!-\!OH$$

1:1 molar ratio   MAP

Scheme 1 Esterification of phosphoric acid with equimolar lauryl alcohol into MAP.

Our experiment results figure that a high yield of 88.5% and selectivity of 93.8% for mono-dodecyl phosphate was achieved with toluene as dehydrant when the direct esterification of phosphoric acid with lauryl alcohol was carried out at 110 ℃ for 24 h under the optimum catalyst dosage of 0.5 % (mass fraction). Above catalytic result is comparable with other inorganic-organic compounds based on poly anions. [32, 33]

Conclusions

The 1D structure of **ε(pyim)₂** is built up of $\{PMo^V_8Mo^{VI}_4O_{38}(OH)_2Zn_4\}$ units modified by pyim organic ligands. To the best of our knowledge, **ε₂(pyim)₆** is the first isolated structural compound in dimeric ε-Zn POMs with good electrochemical properties and high catalytic activity in esterification constructed of eight-reduced ε-keggin cores. The different structures of **ε(pyim)₂** and **ε₂(pyim)₆** demonstrate that the slight differences of the pH in the synthesis conditions can lead to a large difference to the structure of the compounds you obtained. The luminescent and electrochemical properties indicate that **ε(pyim)₂** and **ε₂(pyim)₆** have a wide range of applications in, e.g., photo or electro catalytic. In additions, the obtaining of **ε(pyim)₂** and **ε₂(pyim)₆** based on pyim ligand is an encouraging step towards the synthesis of a new family of POMOFs linked by pyim ligands.

Acknowledgements

References

1   D.L. Long, R. Tsunashima and L. Cronin, *Angew. Chem., Int. Ed*., 2010, **49**, 1736.

2   A. Müller, F. Peters, M. T. Pope and D. Gatteschi, *Chem. Re*v., 1998, **98**, 239.

3   J. Lee, O. K. Farha, J. Roberts, K. Scheidt, S. T. Nguyena and J. T Hupp, *Chem. Soc. Rev.*, 2009, **38**, 1450.

4   Y. Xu, K. L. Zhang, Y. Zhang, X. You and J. Q. Xu, *Chem. Commun.*, 2000, **2**, 153.

5   A. Dolbecq, E. Dumas, C. R. Mayer and P. Mialane, *Chem. Rev.*, 2010, **110**, 6009.

6   J. T. Rhule, C. L. Hill, D. A. Judd and R. F. Schinazi, *Chem. Rev.*, 1998, **98**. 327.

7   A. Tripathi, T. Hughbanks and A. Clearfield, *J. Am. Chem. Soc.*, 2003, **125**, 10528.

8   L. Chen, J. Y. Guo, X. Xu, W. W. Ju, D. Zhang, D. R. Zhu and Y. Xu, *Chem Commun.*, 2013, **49**, 9728.

9   P. Mialane, A. Dolbecq, L. Lisnard, A. Mallard, J. Marrot and F. Sécheresse, *Angew. Chem., Int. Ed.*, 2002, **41**, 2398.

10 L. C. W. Baker and J. S. Figgis, *J, Am. Chem. Soc.*, 1970, **92**, 3794.

11 M. Eddaoudi, D. B. Moler, H. L. Li, B. L. Chen, M. O'Keeffe and O. M. Yaghi, *Acc. Chem. Res.*, 2001, **34**, 319.

12 J. Y. Guo, X. Jin, L. Chen, Z. Wang and Y. Xu, *J. Coord. Chem.*, 2012, **65**, 3821.

13 X. K. Fang, T. M. Anderson and C. L. Hill, *Angew. Chem., Int. Ed.*, 2005, **44**, 3540.

14 C. Lei, J. G. Mao, Y. Q. Sun and J. L. Song, *Inorg. Chem.*, 2004, **43**, 1964-1968.

15 A. Dolbecq, C. Mellot-Draznieks, P. Mialane, J. Marrot, G. Férey and F. Sécheresse, *Eur. J. Inorg. Chem.*, 2005, **2005**, 3009.

16 W. Wang, L. Xu, G. Gao, L. Liu and X. Liu, *CrystEngComm.*, 2009, **11**, 2488.

17 L. M. Rodriguez-Albelo, A. R. Ruiz-Salvador, A. Sampieri, D. W. Lewis, A. Gómez, B. Nohra, P. Mialane, J. Marrot, F. Sécheresse, C. Mellot-Draznieks, R. Ngo. Biboum, B. Keita, L. Nadjo and A. Dolbecq, *J. Am. Chem. Soc.*, 2009, **131**, 16078.

18 L. M. Rodriguez-Albelo, A. R. Ruiz-Salvador, D. L. Lewis, A. Gómez, P. Mialane, J. Marrot, A. Dolbecq, A. Sampieri and C. Mellot-Draznieks, *Phys. Chem. Chem. Phys.*, 2010, **12**, 8632.

19 B. Nohra, H. El-Moll, L. M. Rodriguez-Albelo, P. Mialane, J. Marrot, C. Mellot-Draznieks, M. O'Keeffe, R. Ngo Biboum, J. Lemaire, B. Keita, L. Nadjo, and A. Dolbecq, *J. Am. Chem. Soc.*, 2011, **133**, 13363.

20 L. M. Rodriguez-Albelo, G. Rousseau, P. Mialane, J. Marrot, C. Mellot-Draznieks, A. R. Ruiz-Salvador, S.W. Li, R. J. Liu, G. J. Zhang, B. Keita and A. Dolbecq, *Dalton Trans*, 2012, **41**, 9989.

21 P. Mialane, A. Dolbecq and F. Sécheresse, *Chem. Commun.*, 2006, 3477.

22 J. M. Clemente-Juan and E. Coronado, *Coord. Chem. Rev.*, 1999, **193–195**, 361.

23 C. M. Liu, D. Q. Zhang and D. B. Zhu, *Cryst. Growth. Des.*, 2003, **3**, 363.

24 A. Doménech, H. García, M. T. Doménech-Carbó, F. Llabrési-Xamena, *J. Phys. Chem. C.*, 2007, **111**, 13701.

25 G. Férey, F. Millange, M. Morcrette, C. Serre, M. L. Doublet, J. M. Grenèche and J. M. Tarascon, *Angew Chem Int Ed.*, 2007, **46**, 3259.

26 B. Chiswell, F. Lion and B. Morris, *Inorg Chem.*, 1964, **3**, 110.

27 A. Dolbecq, P. Mialane, L. Lisnard, J. Marrot and F. Sécheresse, *Chem A Eur J.*,

2003, **9**, 2914.

28 W. J. Wang, L. Xu, G. G. Gao, L. Liu and X. Z. Liu, *CrystEngComm.*, 2009, **11**, 2488.

29 B. X. Wang and S. J. Dong, *Electrochim Acta.*, 1992, **37**, 1859.

30 P. Wang, X. P. Wang and G. Y. Zhu, *Electrochim Acta.*, 2001, **46**, 637.

31 L. P. Zhao and L. J. Zhao, *Guangxi Chemical Industry.*, 2000, **29**, 46.

32 L. Shen, Y. Len, J. Wang and Xu Y. *Chinese Journal of Catalysis.*, 2010, **31**, 156.

33 H. Miao, X. Xu, W. Ju, H. Wan, Y. Zhang, D. and Y. Xu, I*norg. Chem.* 2014, **53**, 2757.

Table 1. Crystal data and structure refinements for **ε(pyim)$_2$** and **ε$_2$(pyim)$_6$**.

Compound	ε(pyim)$_2$	ε$_2$(pyim)$_6$
formula	C$_{32}$H$_{34}$Mo$_{24}$N$_{12}$Na$_2$O$_{83}$ P$_2$Zn$_8$	C$_{24}$H$_{25}$Mo$_{12}$N$_9$O$_{42}$PZn$_4$
fw	4848.15	2555.26
T (K)	296(2) K	296(2) K
Wavelength (Å)	0.71073 A	0.71073 A
cryst syst	triclinic	monoclinic
space group	P$\bar{1}$	P2$_1$/c
a (Å)	a = 13.138(2)	13.571(3)
b (Å)	b = 14.569(2)	23.527(4)
c (Å)	c = 14.778(2)	18.041(3)
α (deg)	61.985(2)	90
β (deg)	87.646(2)	106.486(2)
γ (deg)	87.263(2)	90

V Å^3	2493.9(7)	5523.6(17)
Z	1	4
Dc (g cm^{-3})	3.228	3.073
μ (mm^{-1})	4.942	4.467
F(000)	2274	4828
Crystal size (mm)	0.15 x 0.13 x 0.12	0.16 x 0.14 x 0.12
θ range (deg)	1.55 ~ 25.50	1.46 ~ 25.50
	-15<=h<=15	-16<=h<=16
Limiting indices	-17<=k<=17	-27<=k<=28
	-17<=l<=17	-20<=l<=21
reflns collected	18375	38125
indep reflns	9087	10197
R(int)	0.0530	0.0950
Data/restraints/params	9087 / 24 / 748	10197 / 0 / 829
GOF	1.024	1.004
R1^a, wR2^b [I>2σ(I)]	0.0425, 0.1058	0.0492, 0.0981
R1, wR2 (all data)	0.0740, 0.1161	0.0952, 0.1105

$^{a}R1 = \Sigma||F_o|-|F_c||/\Sigma|F_o|.$ $^{b}wR2 = \Sigma[w(F_o^2-F_c^2)^2]/\Sigma[w(F_o^2)^2]^{1/2}.$
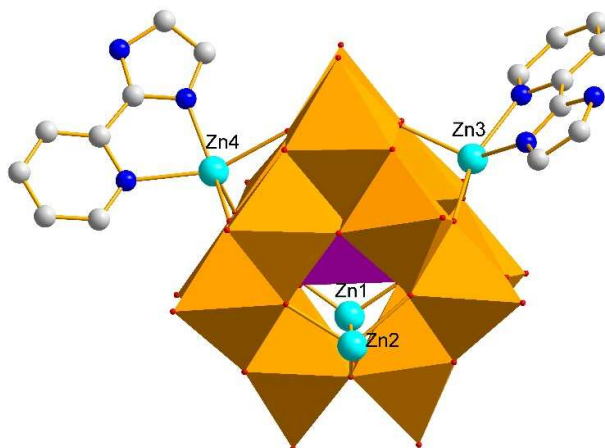
Figure 1. Ball-and-stick and polyhedral view of the asymmetric unit of **ε(pyim)₂**. The hydrogen

atoms, sodium atom and crystal water molecules are omitted for clarity.
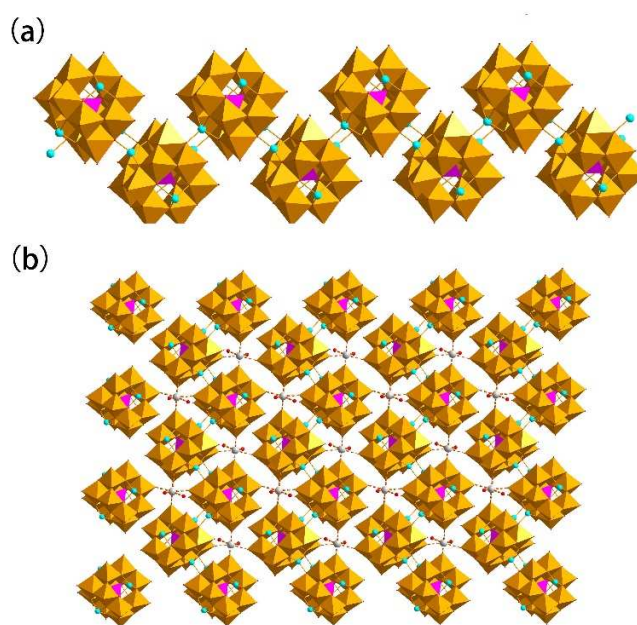
Figure 2. (a) Representation of the 1D structure in **ε(pyim)₂**. (**b**) The layer structure in **ε(pyim)₂**.
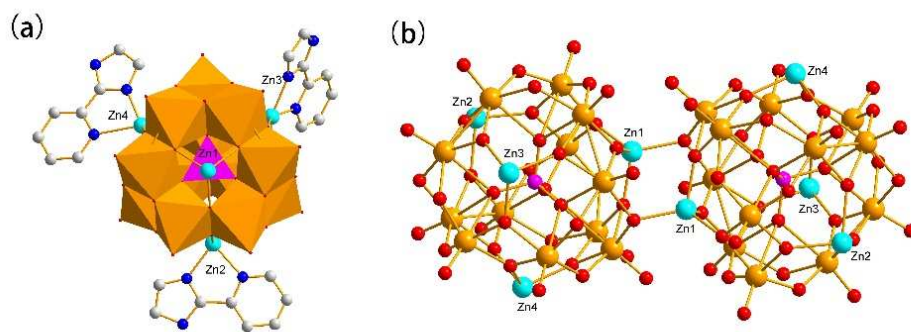
Figure 3. (a) Ball-and-stick and polyhedral view of the basic unit in $\varepsilon_2(\text{pyim})_6$. **(b)** The dimeric ε-Zn Keggin unit in $\varepsilon_2(\text{pyim})_6$. The hydrogen atoms and crystal water molecules are omitted for clarity.
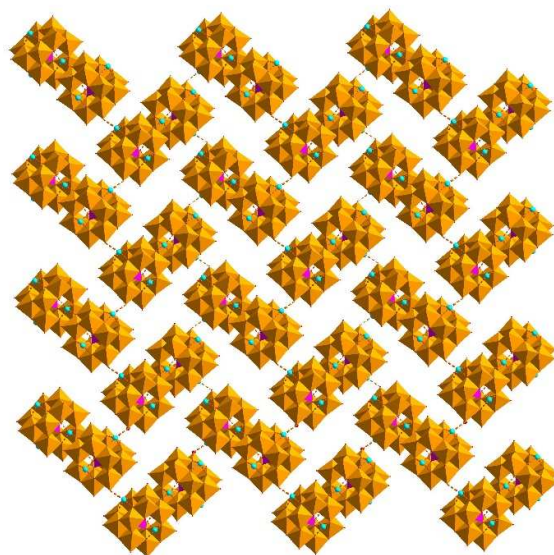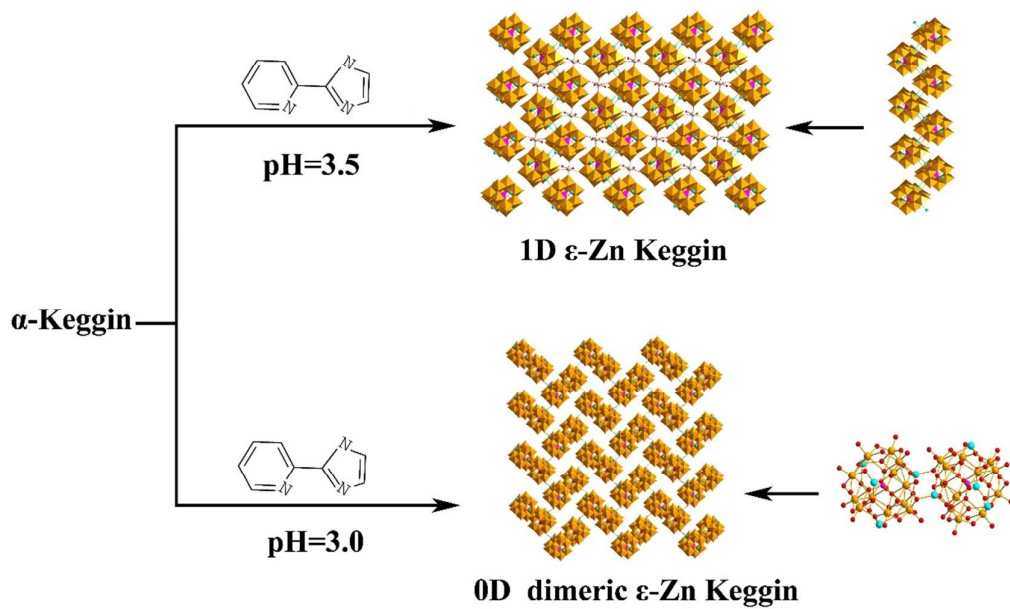

Figure 4. The layer structure in $\varepsilon_2(\text{pyim})_6$.
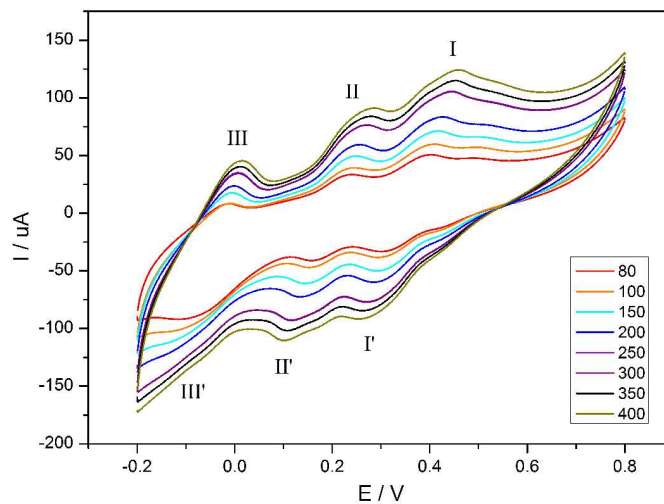
Figure 5. Cyclic voltammograms of the **ε(pyim)₂**–CPE in a 1 M H_2SO_4 aqueous solution at different scan rates (from inner to outer: 80, 100, 150, 200, 250, 300, 350, 400 mV s^{-1})
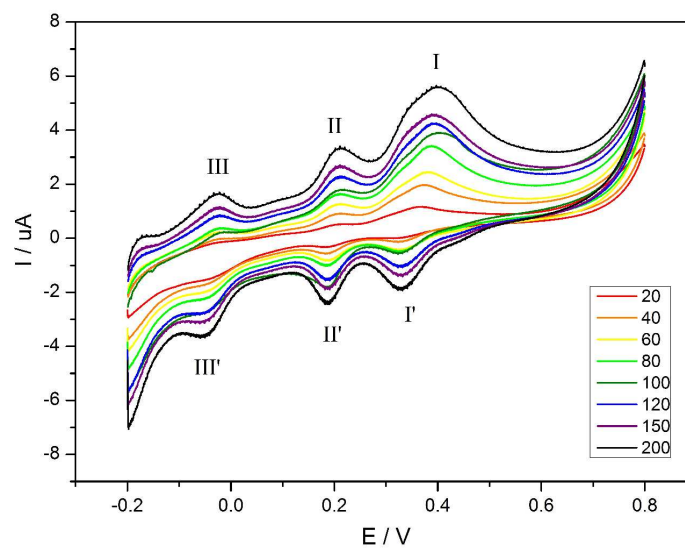
Figure 6. Cyclic voltammograms of the **ε₂(pyim)₆**–CPE in a 1 M H_2SO_4 aqueous solution at different scan rates (from inner to outer: 20, 40, 60, 80, 100, 120, 150, 200 mV s^{-1})

Two novel hybrids **ε(pyim)₂** and **ε₂(pyim)₆**, based on ε-Zn Keggin units have been synthesized under hydrothermal conditions by controlling pH values.